1-29-2015

Building And Testing Correlations For The Estimation Of One-electron Reduction Potentials Of A Diverse Set Of Organic Molecules

Dalvin D. Méndez-Hernández

Jason G. Gillmore
Hope College, gillmore@hope.edu

Luis A. Montano

Devens Gust

Thomas A. Moore

See next page for additional authors

Recommended Citation

Authors
Dalvin D. Méndez-Hernández, Jason G. Gillmore, Luis A. Montano, Devens Gust, Thomas A. Moore, Ana L. Moore, and Vladimiro Mujica

Building and Testing Correlations for the Estimation of One-electron Reduction Potentials of a Diverse Set of Organic Molecules.

Dalvin D. Méndez-Hernández*,§,[1] Jason G. Gillmore*,[1,2] Luis A. Montano,[1] Devens Gust,[1] Thomas A. Moore,[1] Ana L. Moore,[1] and Vladimiro Mujica[1]

1) Center for Bio-Inspired Solar Fuel Production, Department of Chemistry and Biochemistry, Arizona State University, Tempe, Arizona 85287-1604

2) Department of Chemistry, Hope College, Holland, Michigan 49423

*Authors to whom correspondence should be addressed.

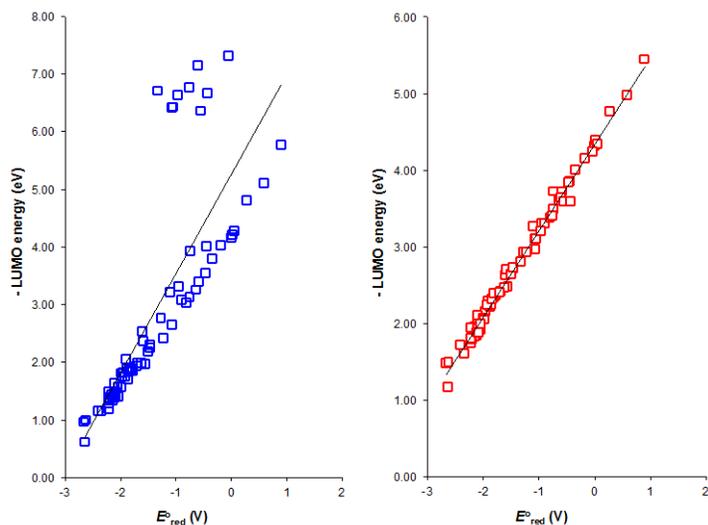E-mail: dalvin.mendez@yale.edu, gillmore@hope.edu

§Present address: Department of Chemistry, Yale University, New Haven, Connecticut 06520-8107

Short Title / Running Head:

TOC Graphic / Graphical Abstract

Short Abstract for TOC

We report on a method for computationally predicting reduction potentials of organic molecules by linearly correlating calculated lowest-unoccupied molecular orbital

(LUMO) energies with experimental ground state reduction potentials. 74 compounds spanning six distinct structural families and a 3.5 V range of reduction potentials were used to build the correlations. This approach is shown to provide a unique combination of computational simplicity and excellent accuracy, even for much larger chromophores and structurally diverse chromophores not included in the correlations.

Abstract

We evaluate a method for computationally predicting reduction potentials of a diverse group of organic molecules by linearly correlating calculated lowest-unoccupied molecular orbital (LUMO) energies with ground state reduction potentials measured in acetonitrile. The approach provides a unique combination of extreme computational simplicity and excellent accuracy across a range of structures and potentials. A disparate set of 74 organic compounds spanning a 3.5 V range of reduction potentials, from six distinct structural families, containing C, H, N, O, F, Cl, and Br, with functional groups including esters, ketones, nitriles, quinones, alkenes, arenes, heteroarenes, and pyridinium and higher benzologs, all containing conjugated pi systems, was used to build the correlations. Varying the basis set used in the B3LYP electronic structure calculations demonstrated only a modest effect of including diffuse functions. It was found that the inclusion of a continuum solvent model in the calculations was required for accurate results, particularly when including cationic species in the correlations (though when only

neutral molecules were examined, reasonable results could even be obtained *in vacuo*).

Several of the best correlations were used to predict the reduction potentials of seven much larger and structurally diverse chromophores that were not included in the correlation data set. Strong correlations (r^2 values > 0.99) with very good predictive abilities (rmsd < 60 mV) were found. This extremely simple and computationally efficient entirely closed-shell methodology is proven robust and useful for the design of new molecules capable of participating in redox processes, including electron transfer reactions.

Introduction

Computational chemistry has become an invaluable tool that can be used in concert with experiment to enable chemists to design improved target molecules by tailoring specific properties[1-8] while potentially minimizing time and material expenses.[9-11] In this context, the role of theory is to construct models that allow the rapid and economical evaluation of the relevant properties and provide guidance to experimentalists. The ability to computationally predict the first redox potentials of compounds is very useful when designing new molecules intended to participate in charge transfer reactions. An excellent recent review by Marenich *et al.* highlights the burgeoning interest in the wide range of approaches to this problem.[12] State-of-the-art calculations of redox potentials using the Born-Haber cycle[5,6,13-21] can provide excellent results, but involve substantial computational work because they require multiple open-shell electronic structure optimizations for radical ions. These open-shell calculations can be computationally expensive, especially for large molecules. In previous work the

Gillmore group has explored the accuracy of this type of calculation using a simplified version of the Born-Haber cycle where the geometry optimizations of the structures (closed shell singlets and one-electron-reduced doublets) were performed in the gas phase, followed by a single-point energy calculation of each structure in the presence of a continuum solvent model.[22,23] This simplified method did not specifically calculate a reduction potential, but something more akin to an electron affinity (albeit in solution). This approach[24] reduces computational cost by avoiding geometry optimization under the constraint of a continuum solvent model and can result in strong empirical correlations between experimentally measured reduction potentials and the calculated energy difference between the molecule and its one-electron reduced product. With proper calibration with a range of known compounds spanning a wide potential window and six diverse structural families, good predictive abilities were achieved. Marenich's recent review[12] seems to indicate that the Gillmore group's most recent work[22] is unique among recent LFER approaches in the breadth of compounds and range of potentials studied.

As an alternative to the Born-Haber cycle methods, linear relationships between molecular orbital energies and the ability of a molecule to accept or donate an electron are among the earliest relationships[25,26] that were considered in the literature and have been used extensively for specific families[27-43] of molecules. The use of a linear correlation of calculated frontier orbital energies (HOMO energy for oxidation, LUMO energy for reduction) of the singlet ground state molecules with their experimentally measured redox potentials is an even simpler way to estimate the redox potentials of unknown molecules. The advantage of this approach is that, in principle, only a single

geometry optimization of the molecule of interest in the initial closed-shell singlet (prior to single electron oxidation or reduction) is required to predict both the experimental first one-electron reduction and oxidation potentials, and all calculations are on closed shell spin paired species. In our recent preliminary report,[27] this strategy was tested with fifty-one polycyclic aromatic hydrocarbons (PAHs) with known oxidation and/or reduction potentials, measured in acetonitrile, and found to be both more accurate and more computationally efficient than the Gillmore group's[22,23] methods.

Although our preliminary report from Arizona State was limited to a single class of organic molecules lacking any functional groups,[27] we nevertheless suspected that this approach might be generally valuable for estimating redox potentials of a more diverse range of structures bearing a variety of functionality. In the present work we have joined forces to apply the purely closed-shell calculations previously reported by the rest of the co-authors for a single set of very similar PAHs to the full range of 74 structurally and functionally diverse compounds (Table 1) spanning a 3.5 V range of reduction potentials and six distinct structural families of compounds previously reported by the Gillmore group[22] at Hope College. We have developed linear correlations between calculated LUMO energies and the reduction potentials of these 74 structurally and functionally diverse molecules. We also report the effects of varying the basis set employed and the inclusion of a dielectric solvent model on the accuracy of the relationships. The resulting correlations were used to accurately predict the experimental reduction potentials of seven additional molecules not used in preparing the correlations. These seven compounds include larger chromophores of up to 82 heavy atoms – four times as large as the largest molecules used to prepare the calibration, and twice as large

as the largest compounds previously reported by Gillmore and coworkers,[22] which had sometimes proved troublesome, or at least extremely time-consuming, when attempting open-shell calculations.

Table 1.   List of compounds (by family), and their experimental reduction potentials,[22] used to build correlations 1-12.

Family/compound number	Compound name	Reduction potential (V vs SCE in acetonitrile)
Cyanoaromatics		
1	tetramethyl-*p*-dicyanobenzene	-1.9
2	*p*-dicyanobenzene	-1.6
3	tetrafluoro-*p*-dicyanobenzene	-1.1
4	tetrachloro-*p*-dicyanobenzene	-0.95
5	1,2,4,5-tetracyanobenzene	-0.74
6	2-cyanonaphthalene	-1.98
7	1-cyano-4-methylnaphthalene	-1.96
8	1-cyanonaphthalene	-1.88
9	1,4-dicyanonaphthalene	-1.27
10	9-cyanoanthracene	-1.58
11	9-cyano-10-phenylanthracene	-1.47
12	9,10-dicyanoanthracene	-0.89
13	3,7,9,10-tetracyanoanthracene	-0.45
Quinones		
14	tetramethyl-*p*-quinone	-0.8
15	trimethyl-*p*-quinone	-0.75
16	2,6-dimethyl-*p*-quinone	-0.63
17	2-methyl-*p*-quinone	-0.58
18	*p*-quinone	-0.47

19	2-chloro-*p*-quinone	-0.34
20	2,6-dichloro-*p*-quinone	-0.18
21	tetrabromo-*p*-quinone	0
22	tetrafluoro-*p*-quinone	0.02
23	tetrachloro-*p*-quinone	0.05
24	2,3-dicyano-*p*-quinone	0.28
25	5,6-dichloro-2,3-dicyano-*p*-quinone	0.59
26	tetracyano-*p*-quinone	0.9
N-Methyl Heteroaromatic Cations		
27	*N*-methylpyridinium	-1.32
28	4-methyl-*N*-methylquinolinium	-1.07
29	2-methyl-*N*-methylquinolinium	-1.05
30	*N*-methylquinolinium	-0.96
31	3-bromo-*N*-methylquinolinium	-0.76
32	3-cyano-*N*-methylquinolinium	-0.6
33	9-phenyl-*N*-methylacridinium	-0.55
34	*N*-methylacridinium	-0.43
35	9-cyano-*N*-methylacridinium	-0.04
Flexible Pi Molecules		
36	diethyl fumarate	-1.5
37	diethyl terephthalate	-1.78
38	benzophenone	-1.86
39	acetophenone	-2.1
40	propiophenone	-2.15
41	*trans*-stilbene	-2.2
42	4-methylacetophenone	-2.2
43	methyl benzoate	-2.22
44	ethyl benzoate	-2.4

Polycyclic Aromatic Hydrocarbons		
45	naphthalene	-2.66
46	acenaphthylene	-1.8
47	cyclopent[fg]acenaphthylene	-1.06
48	anthracene	-2.1
49	phenanthrene	-2.62
50	aceanthrylene	-1.47
51	acephenanthrylene	-1.81
52	fluoranthene	-1.92
53	pyrene	-2.22
54	benzo[ghi]fluoranthene	-1.84
55	dibenzo[ghi,mno]fluoranthene	-1.99
56	perylene	-1.81
Heterocyclic amines		
57	benzo[c]cinnoline	-1.554
58	cinnoline	-1.686
59	phthalazine	-1.976
60	phenanthridine	-2.118
61	pyridazine	-2.12
62	pyrimidine	-2.34
63	benzo[f]quinoline	-2.14
64	benzo[h]quinoline	-2.208
65	isoquinoline	-2.22
66	*o*-phenanthroline	-2.042
67	*m*-phenanthroline	-2.092
68	*p*-phenanthroline	-2.044
69	pyridine	-2.636
70	quinoline	-2.105

71	acridine	-1.62
72	pyrazine	-2.08
73	phenazine	-1.227
74	quinoxaline	-1.702

Results and discussion

Linear correlations were constructed by plotting the calculated LUMO energy (eV) of each molecule as a function of its corresponding experimental reduction potential (V vs SCE) measured in acetonitrile. The LUMO energies were obtained by three different means: 1) directly from a geometry optimization of the molecules in the gas phase, 2) from a single-point energy calculation of that gas-phase geometry in the presence of solvent, or 3) from a geometry optimization in the presence of the solvent. These calculations were all performed using theB3LYP hybrid functional with either the 6-31G(d) or 6-311+G(2d,p) basis sets. A summary of the resulting parameters for the correlations studied can be found in Tables 2 and 3.

Table 2. Correlations of Calculated LUMO Energies with Experimental Reduction Potentials for Compounds 1−74, Varying Computational Methodology.

Corr. #	Method/ basis set	Calculation type/ solvent model[a]	slope m (eV/V)	y-intercept b (eV)	r^2	rmsd[b] residuals (V)	MAD[c] residuals (V)	x-intercept (V)
1	B3LYP/ 6-31G(d)	Opt/gas	1.7213	5.2616	0.6276	0.6276	0.3985	-3.0568
2	B3LYP/ 6-311+G(2d,p)	Opt/gas	1.6615	5.5212	0.6277	0.6331	0.3967	-3.3230
3	B3LYP/ 6-31G(d)	Sp/CPCM	1.1844	4.0873	0.9903	0.0815	0.0644	-3.4509

Corr. #	Method	Calculation type/ solvent model[a]	slope m (eV/V)	y-intercept b (eV)	r^2	rmsd[b] residuals (V)	MAD[c] residuals (V)	x-intercept (V)
4	B3LYP/ 6-311+G(2d,p)	Sp/CPCM	1.1291	4.3340	0.9917	0.0753	0.0579	-3.8385
5	B3LYP/ 6-31G(d)	Opt/CPCM	1.1825	4.0882	0.9908	0.0791	0.0614	-3.4573
6	B3LYP/ 6-311+G(2d,p)	Opt/CPCM	1.1275	4.3372	0.9918	0.0749	0.0589	-3.8467

[a]Opt = optimization, Sp = single-point, gas = gas phase calculations, CPCM = calculation using the Conductor-like Polarizable Continuum Model (with acetonitrile as solvent). [b]Root mean square deviation, taken from individual residuals for each compound as predicted by each trend line (as reported in the Supporting Information). [c]Mean average deviation, taken from individual residuals for each compound as predicted by each trend line (as reported in the Supporting Information).

Table 3. Correlations of Calculated LUMO Energies with Experimental Reduction Potentials for Compounds 1−26 and 36-74 (Excluding the *N*-Methyl Heteroaromatic Cations family 27-35) Varying Computational Methodology.

Corr. #	Method	Calculation type/ solvent model[a]	slope m (eV/V)	y-intercept b (eV)	r^2	rmsd[b] residuals (V)	MAD[c] residuals (V)	x-intercept (V)
7	B3LYP/ 6-31G(d)	Opt/gas	1.3415	4.3129	0.9776	0.1252	0.0935	-3.2150
8	B3LYP/ 6-311+G(2d,p)	Opt/gas	1.2947	4.6055	0.9748	0.1330	0.0994	-3.5572
9	B3LYP/ 6-31G(d)	Sp/CPCM	1.1837	4.0825	0.9901	0.0826	0.0641	-3.4489
10	B3LYP/ 6-311+G(2d,p)	Sp/CPCM	1.1399	4.3583	0.9923	0.0729	0.0580	-3.8234
11	B3LYP/ 6-31G(d)	Opt/CPCM	1.1840	4.0887	0.9907	0.0801	0.0618	-3.4533
12	B3LYP/ 6-311+G(2d,p)	Opt/CPCM	1.1411	4.3679	0.9928	0.0702	0.0559	-3.8278

For the correlations that include all 74 compounds (Table 1), the correlations obtained from gas phase geometry optimizations (1-2) resulted in very low r^2, as had been previously noted,[22] whereas when the solvent was included either in a single-point energy calculation (5-8) or a full geometry optimization (9-12) the r^2 approached the optimal value of 1. This difference is due primarily to greater underestimation of the LUMO energies for the family of *N*-methyl heteroaromatic cations calculated in the gas phase, which is corrected once the solvent (acetonitrile) is included using the Conductor-like Polarizable Continuum Model (CPCM).[44,45] Figure 1 illustrates some of the correlations from Table 2.
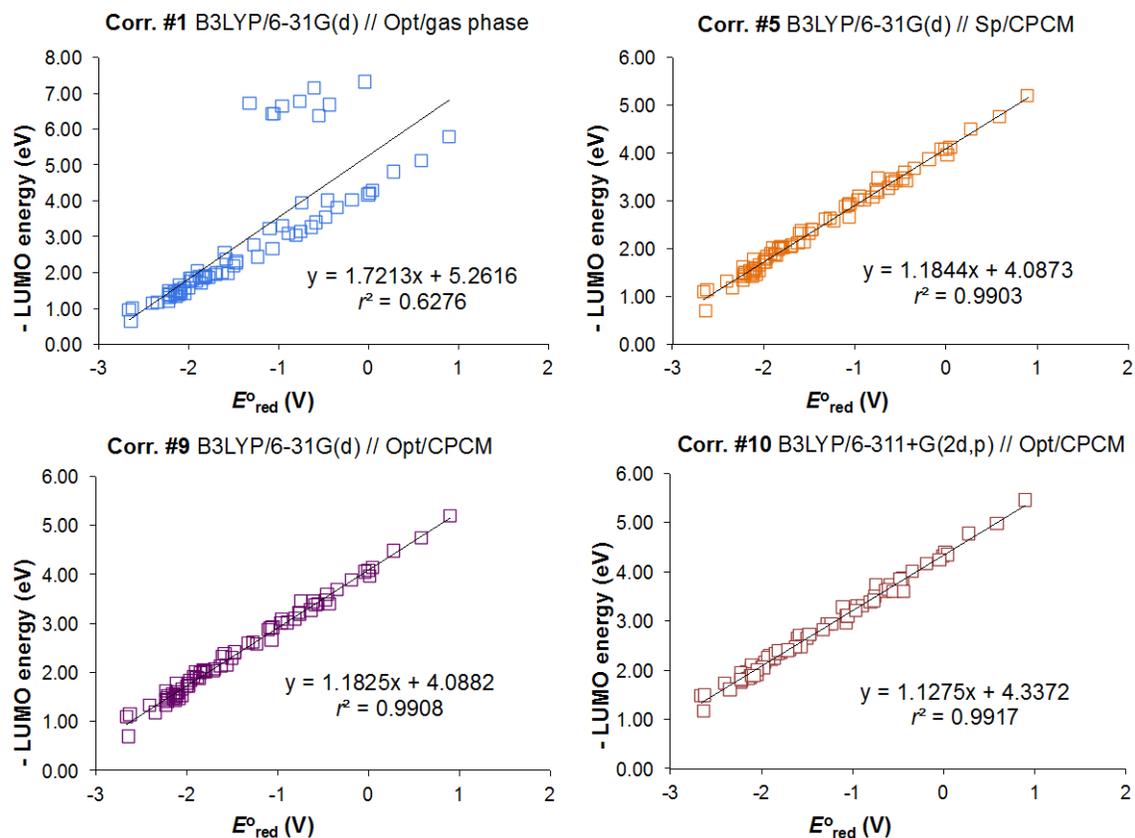
Figure 1. Plots of Selected Correlations from Table 2.

In order to compare the three computational approaches without the difficulty imposed by the inclusion of closed-shell cations in the correlation which are more susceptible to solvent stabilization, new correlations were built with only sixty-three of the seventy-four compounds, spanning five structural families and omitting the *N*-methyl heteroaromatic cations, and the results are shown in Table 3. The r^2 improved for all the correlations in Table 3 (7-12) when compared to those in Table 2 (1-6). This is, as expected, especially evident for correlations based upon gas phase energies (7-8 vs. 1-2), where the *N*-methyl heteroaromatic cations had proved problematic in the gas phase. Gas-phase correlations of gas-phase LUMO energies vs. experimental reduction

potentials of 65 compounds spanning 5 families of neutral organic compounds with $r^2 >$ 0.97 and MAD < 100 mV (rmsd < 135 mV) are possible. This is a 4- to 5-fold improvement over gas-phase correlations that included the N-Methylheteroaromatic cations **27-35**. Nevertheless, as with correlations 1-6 that included compounds **27-35**, the r^2 for correlations 7-12 still increased when the solvent was included either in a single-point energy calculation or a full geometry optimization. Given the computational cost savings of our present method only requiring a single closed-shell calculation, the added cost of a single CPCM calculation can generally easily be absorbed and is advisable wherever feasible. It was also observed that the rmsd for individual families was in general just slightly better than for the global correlations (see Supporting Information), indicating that when a correlation is available for an exact family of molecules, the correlation is particularly good for that family; however the almost equally good global correlations clearly indicate that good predictive ability should be able to be obtained even for molecules not necessarily well represented structurally in the initial correlation, just as the Gillmore group noted for their prior method.[22,23]

Slope and intercepts

The correlations in Tables 2 and 3 were built with the experimental reduction potentials on the *x*-axis because this was the control variable as the correlations were built, and also to be consistent with our previous work.[22,23,27] In the Gillmore group's prior methodology,[22,23] the energy difference between the initial closed-shell singlet and one-electron reduced doublet states was used as an analog to an electron affinity in a dielectric continuum rather than the gas phase. Thus to the extent that this was equivalent to a reduction potential, the slope should have approached unity and the *x*- and *y*-

intercepts the reference potential relative to which the literature reduction potentials were reported in V vs SCE or eV vs vacuum, respectively. Even in this previous (and more computationally expensive) methodology, deviation from a slope of 1.0 was observed in the best predictive correlations. This is indicative of fitting parameters that accommodate systemic error while preserving good correlation and accurate predictive ability. The present work makes improvements in both predictive ability and computational efficiency. Specifically MAD (mean absolute deviation), rmsd (root mean squared deviation), and r^2 all improved while the number of calculations and overall compute time both decreased significantly, indicative of gains in both efficiency and accuracy of the present linear correlation methodology with closed-shell LUMO energy calculations, over trying to compute an actual reduction potential or even model it with an electron affinity.   Meanwhile the slope and intercepts in the present correlations, somewhat surprisingly, are similar to those obtained previously and get closer to the values that might be expected for more direct computation of reduction potentials when solvent is included. Agreement is further improved (though only modestly) when the larger basis set with diffuse functions is used. These last results are interesting and not necessarily expected, as the present method is less clearly related to a direct computation of reduction potential. These results may indicate either a fortuitous cancellation of errors with this particular combination of computational parameters, or that the LUMO energy itself (in the presence of a solvent model and with the inclusion of diffuse functions) is indeed rather closely related to absolute reduction potential. A thorough investigation of this effect is beyond the scope of our present work.

Testing the correlations

After building the correlations 1-12, some of the best correlations were tested to see how well they would predict the reduction potentials of seven compounds that were not included in the correlation data set, in order to provide a true test of the predicting ability of the methodology: two perimidinespirohexadienone (PSHD) photochromes and their long-wavelength quinonimine isomers (**75-78**),[22] and three perylene dianhydrides[46] (**79-81**). These compounds are examples of chromophores our groups have previously explored as potential photoinduced charge transfer initiators.
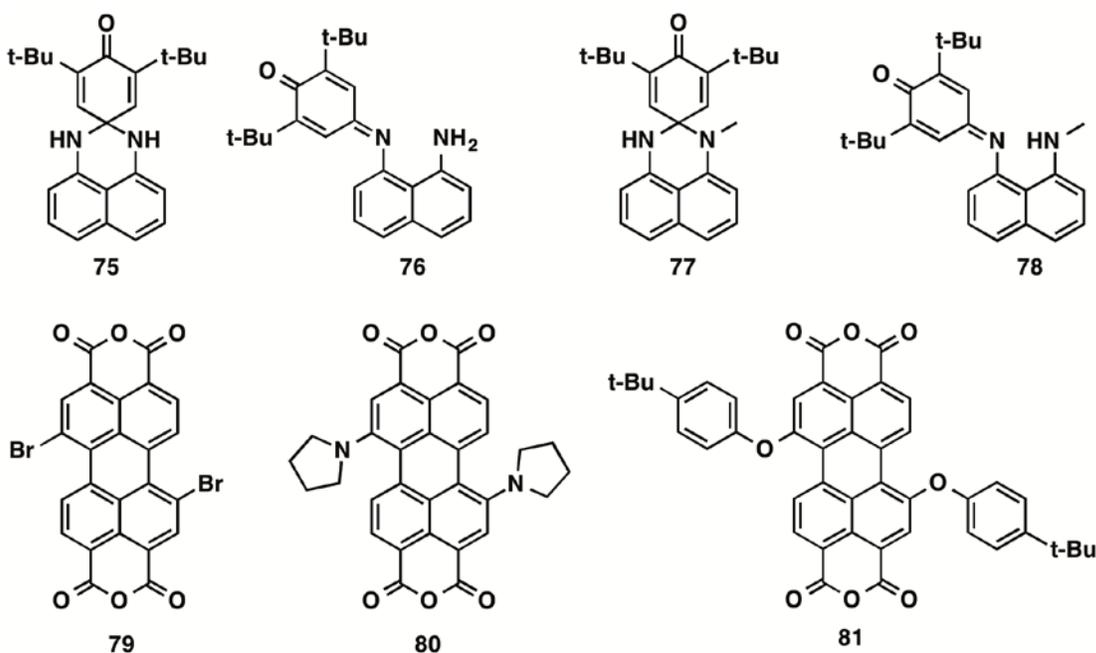
Correlations performed with density functional theory (DFT) resulted in an improved r^2 and in lower rmsd and MAD values than the correlations performed with semi-empirical methods (included in the SI). The DFT correlations were tested further with molecules **75-81**. Table 4 shows the reduction potentials calculated by linear extrapolation from the DFT correlations for these seven compounds. In general, correlations and 6 and 9 yielded better results (~ 10 mV lower rmsd) than correlation 5.

Therefore, geometry optimization in the presence of the solvent or using a higher-level basis set seems to be modestly beneficial, but results in an increase of the overall computation time. Correlation 10 yielded only similar rmsd to those of correlations 6 and 9, while being a more expensive calculation by involving both geometry optimization in the presence of the solvent and the use of a higher-level basis set.

Table 4. Comparison of Experimental Reduction Potentials of Four PSHD Photochromes and Two Perylenes to Those Predicted Using Selected Correlations.

Compound	Exptl E^{o}_{red} (V vs SCE in acetonitrile)	Predicted E^{o}_{red} (V vs SCE)			
		Corr. 5	Corr. 6	Corr. 9	Corr. 10
75	-1.74	-1.69	-1.76	-1.68	-1.77
76	-0.94	-0.89	-0.96	-0.89	-0.97
77	-1.68	-1.68	-1.76	-1.67	-1.77
78	-0.94	-0.89	-0.95	-0.89	-0.97
79	-0.25	-0.33	-0.32	-0.30	-0.28
80	-0.72	-0.78	-0.78	-0.77	-0.75
81	-0.51	-0.55	-0.54	-0.53	-0.51
rmsd[a]	-	0.05	0.04	0.04	0.04
MAD[b]	-	0.05	0.04	0.04	0.03

[a]Root mean square deviation, taken from individual residuals for each compound as predicted by each trend line (as reported in the Supporting Information). [b]Mean average deviation, taken from individual residuals for each compound as predicted by each trend line (as reported in the Supporting Information).

Correlations with all 81 compounds

The correlations of the experimental one-electron reduction potential of all eighty-one compounds, thus including the seven additional larger "test" compounds along with the original 74 calibrants, with their calculated LUMO energy determined with different methodologies are shown in Table 5. It is important to note that for the correlations on this table the axes have been switch by plotting experimental reduction (V vs SCE) vs. LUMO energies (eV), thus transposing the x- and y-axes of our correlations, as the predicted redox potential is now the value of interest. These correlations (13-16) are illustrated in Figure 2.
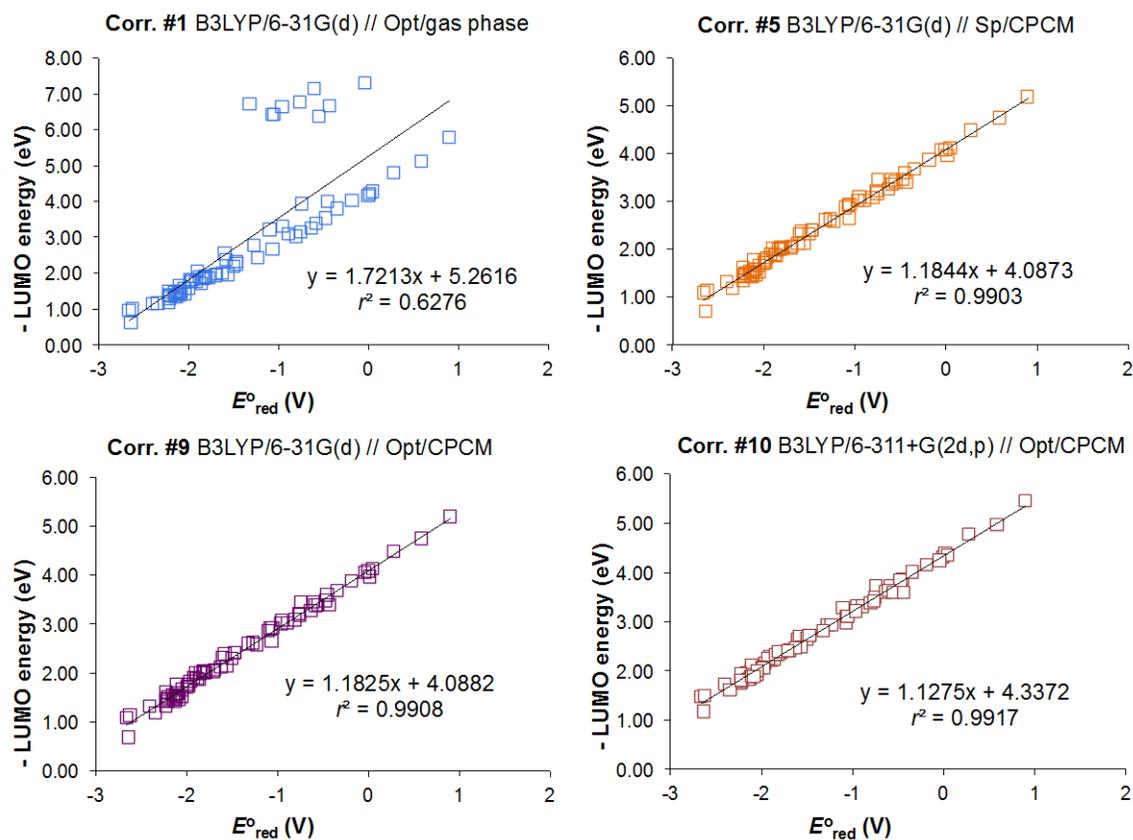
Table 5. Correlations of Experimental Reduction Potential with calculated LUMO Energies for Compounds 1−81, Varying Computational Methodology.

Corr. #	Method	Calculation type/ solvent model[a]	slope m (V/eV)	y-intercept b (V)	r^2	rmsd[b] residuals (V)	MAD[c] residuals (V)
13	B3LYP/ 6-31G(d)	Sp/CPCM	0.8386	-3.4364	0.9905	0.0791	0.0628
14	B3LYP/ 6-311+G(2d,p)	Sp/CPCM	0.8807	-3.8209	0.9919	0.0731	0.0562
15	B3LYP/ 6-31G(d)	Opt/CPCM	0.8395	-3.4426	0.9911	0.0764	0.0594
16	B3LYP/ 6-311+G(2d,p)	Opt/CPCM	0.8805	-3.8263	0.9921	0.0722	0.0562

[a]Opt = optimization, Sp = single-point, gas = gas phase calculations, CPCM = calculation using the Conductor-like Polarizable Continuum Model (with acetonitrile as solvent). [b]Root mean square deviation, taken from individual residuals for each compound as predicted by each trend line (as reported in the Supporting Information). [c]Mean average

deviation, taken from individual residuals for each compound as predicted by each trend line (as reported in the Supporting Information).

Figure 2. Plots of Selected Correlation from Table 5.

Conclusions

We have shown that a strong linear correlation between computed LUMO energies and experimental reduction potentials can be obtained for a large series of diverse organic compounds with very different structures and substituents spanning a range of more than 3.5 V of reduction potentials. The use of a solvent model in the calculations (either in the full geometry optimization, or as a single-point calculation on

the gas phase optimized geometries) significantly improves the quality of the correlation, resulting in lower rmsd values than for the gas phase correlations. This was particularly true when the *N*-methyl heteroaromatic cations were included in the correlations (1-6).

The main drawback of this methodology is the need to construct a linear correlation previous to being able to make predictions. However the correlations (13-16) reported herein appear sufficiently robust to allow prediction of the first reduction potentials of molecules structurally and functionally distinct from those used to calibrate the correlation, including those like the PSHDs (**75-78**) that do not neatly fit into any of the typical families of structures. We do however note that our calibrant molecules, while broadly diverse, do consist solely of relatively rigid organics (though **36-44** were chosen to add at least modest conformational flexibility) with conjugated pi systems, thus yielding delocalized open-shell species upon reduction. Furthermore only molecules containing C, H, N, O, F, Cl, and Br are represented, with functional groups including esters, ketones, halides, nitriles, quinones, alkenes, arenes, heteroarenes, and pyridinium and higher benzologs. Additional correlations in different solvents or based upon different families of compounds or functional groups can be developed by individual users or by the broader community, as there is need or interest. These will of course depend on the availability (or measurement) of appropriate experimental redox potential data for those compounds in those solvents.

A comparison of the best correlation that includes all seventy-four compounds from Gillmore's previous work (r^2 = 0.9889, rmsd = 0.0829 V) with the best correlation from this work (r^2 = 0.9918, rmsd = 0.0749 V) shows a modest but meaningful improvement in accuracy, and a significant improvement in computational efficiency. As

mentioned in the Introduction, the main advantage of the methodology used in this work is that it requires only closed-shell calculations, thereby reducing both the number and complexity of calculations required. Prior work required gas phase geometry optimizations of two different species, and then calculation of their single-point energies in the presence of solvent.[22,23] The present work can be completed with a single geometry optimization (with or without solvent), and the energy of the gas phase geometry can be improved by a single-point energy calculation with solvent. Based on our results, performing gas phase geometry optimizations followed by single-point energy calculations on the gas phase geometries in the presence of a continuum solvent model is recommended for a good balance of accuracy and calculation time when building MO-redox correlations.

The methodology studied in this work is useful for predicting reduction potentials when designing new molecules, and is computationally less expensive than Gillmore's[22,23] previous method. Moreover, based on our prior work, which was limited to PAHs but studied oxidation as well as reduction potentials,[27] it is expected that this approach should be similarly generalizable to correlations of HOMO energies to oxidation potentials across a wide range of structures and potentials. Future work in our group will include using the present correlations to predict reduction potentials of porphyrins and phthalocyanines, and developing additional correlations in different solvents and with additional calibration molecules (perhaps including porphyrins and phthalocyanines) including correlations of HOMO energies with oxidation potentials as well as LUMO energies with reduction potentials.

Computational Methodology

A series of 74 compounds (listed in the SI) were submitted to the following procedure:

1) Geometry optimization in gas phase (Corr. 1, 2, 7 and 8), followed by

2) Single-point energy calculation in solvent model (Corr. 3, 4, 9 and 10) or

3) Geometry optimization in solvent model (Corr. 5, 6, 11 and 12)

The B3LYP[47,48] hybrid density functional was used throughout. Two different basis sets were tested: B3LYP/6-31G(d) and B3LYP/6-311+G(2d,p).[49-51] All compounds were geometry optimized using *Gaussian 09*.[52] For the calculations that involved the presence of solvent (acetonitrile) the Conductor-like Polarizable Continuum Model (CPCM) was employed.[44,45] The calculated LUMO energy for each molecule was plotted against the experimental one-electron reduction potential. The experimental reduction potentials were taken from the literature.[22] The literature potentials were measured in acetonitrile and are reported in V vs. SCE, after correction from other reference electrodes as necessary.

Supporting Information

An Excel workbook with separate tabbed worksheets for each basis set and methodology combination, providing additional graphs and correlations by family of molecules as well as all correlations reported herein, and including complete data of the individual computed LUMO energies for each molecule at each level of theory, along with the literature reduction potentials to which they were correlated, and a separate PDF document containing particularly relevant data tables extracted from the Excel workbook,

along with the Cartesian coordinates of molecules **1-81** optimized at the B3LYP/6-311+G(2d,p) level of theory using CPCM to simulate acetonitrile.

References

[1]   D.P. Hagberg, J.-H. Yum, H. Lee, F. De Angelis, T. Marinado, K.M. Karlsson, R. Humphry-Baker, L. Sun, A. Hagfeldt, M. Grätzel, M.K. Nazeeruddin, *J. Am. Chem. Soc.* **2008**, *130*, 6259.
[2]   D.P. Hagberg, T. Marinado, K.M. Karlsson, K. Nonomura, P. Qin, G. Boschloo, T. Brinck, A. Hagfeldt, L. Sun, *J. Org. Chem.* **2007**, *72*, 9550.
[3]   C.-W. Lee, H.-P. Lu, C.-M. Lan, Y.-L. Huang, Y.-R. Liang, W.-N. Yen, Y.-C. Liu, Y.-S. Lin, E.W.-G. Diau, C.-Y. Yeh, *Chem. Eur. J.* **2009**, *15*, 1403.
[4]   J.S. Meisner, D.F. Sedbrook, M. Krikorian, J. Chen, A. Sattler, M.E. Carnes, C.B. Murray, M. Steigerwald, C. Nuckolls, *Chem. Sci.* **2012**, 3, 1007.
[5]   S.J. Konezny, M.D. Doherty, O.R. Luca, R.H. Crabtree, G.L. Soloveichik, V.S.

Batista, *J. Phys. Chem. C* **2012**, *116*, 6349.

[6]   C.E. Crespo-Hernández, D.M. Close, L. Gorb, J. Leszczynski, *J. Phys. Chem. B* **2007**, *111*, 5386.

[7]   T. Arslan, F. Kandemirli, E.E. Ebenso, I. Love, H. Alemu, *Corros. Sci.* **2009**, *51*, 35.

[8]   R. Ma, P. Guo, H. Cui, X. Zhang, M.K. Nazeeruddin, M. Grätzel, *J. Phys. Chem. A* **2009**, *113*, 10119.

[9]   R. Olivares-Amaya, C. Amador-Bedolla, J. Hachmann, S. Atahan-Evrenk, R.S. Sánchez-Carrera, L. Vogt, A. Aspuru-Guzik, *Energy Environ. Sci.* **2011**, *4*, 4849.

[10]   U. F. Röhrig, S. R. Majjigapu, M. Chambon, S. Bron, L. Pilotte, D. Colau, B.J. Van den Eynde, G. Turcatti, P. Vogel, V. Zoete, O. Michielin *Eur J Med Chem* **2014**, *84*, 284.

[11]   D. Xiao, L. A. Martini, R. C. Snoeberger, R. H. Crabtree, V. S. Batista *J. Am. Chem. Soc.* **2011**, *133*, 9014.

[12]   A.V. Marenich, J. Ho, M.L. Coote, C.J. Cramer, D.G. Truhlar, *Phys. Chem. Chem. Phys.* **2014**, *16*, 15068.

[13]   C.A. Reynolds, P.M. King, W.G. Richards, *Nature* **1988**, *334*, 80.

[14]   L.E. Roy, E. Jakubikova, M.G. Guthrie, E.R. Batista, *J. Phys. Chem. A* **2009**, *113*, 6745.

[15]   M. Namazian, M.L. Coote, *J. Phys. Chem. A* **2007**, *111*, 7227.

[16]   X.-L. Li, Y. Fu, *J. Mol. Struct.: THEOCHEM* **2008**, *856*, 112.

[17]   J. Shi, Y.-L. Zhao, H.-J. Wang, L. Rui, Q.-X. Guo, *J. Mol. Struct.: THEOCHEM* **2009**, *902*, 66.

[18]   A.P. Davis, A.J. Fry, *J. Phys. Chem. A* **2010**, *114*, 12299.

[19]   J.M. Villegas, S.R. Stoyanov, W. Huang, D.P. Rillema, *Inorg. Chem.* **2005**, *44*, 2297.

[20]   T. Tugsuz, *J. Phys. Chem. B* **2010**, *114*, 17092.

[21]   D.H. Evans, *Chem. Rev.* **2008**, *108*, 2113.

[22]   E.J. Lynch, A.L. Speelman, B.A. Curry, C.S. Murillo, J.G. Gillmore, *J. Org. Chem.* **2012**, *77*, 6423.

[23]   A.L. Speelman, J.G. Gillmore, *J. Phys. Chem. A* **2008**, *112*, 5684.

[24]   P. Winget, C. J. Cramer, D. G. Truhlar *Theoret. Chim. Acta* **2004**, *112*, 217.

[25]   A. Maccoll, *Nature* **1949**, *163*, 178.

[26]   T. Koopmans, *Physica* **1934**, *1*, 104.

[27]   D.D. Méndez-Hernández, P. Tarakeshwar, D. Gust, T.A. Moore, A.L. Moore, V. Mujica, *J. Mol. Model.* **2012**, *19*, 2845.

[28]   A.J. Fry, P.C. Fox, *Tetrahedron* **1986**, *42*, 5255.

[29]   G. Sereda, J. Van Heukelom, M. Koppang, S. Ramreddy, N. Collins, *Beilstein J. Org. Chem.* **2006**, *2*, 26.

[30]   J. Casado, M.C. Ruiz Delgado, M.C. Rey Merchán, V. Hernández, J.T. López Navarrete, T.M. Pappenfus, N. Williams, W.J. Stegner, J.C. Johnson, B.A. Edlund, D.E. Janzen, K.R. Mann, J. Orduna, B. Villacampa, *Chem. Eur. J.* **2006**, *12*, 5458.

[31]   S. Jameh-Bozorghi, A. Mansouri, B. Dadpou, *Int. J. Electrochem.* **2010**, *5*, 867.

[32]   A. Kuhn, K.G. Von Eschwege, J. Conradie, *Electrochimica Acta* **2011**, *56*, 6211.

[33]   K.G. Von Eschwege, J. Conradie, *S. Afr. J. Chem.* **2011**, *64*, 203.

[34]   C. Koper, M. Sarobe, L.W. Jenneskens, *Phys. Chem. Chem. Phys.* **2004**, *6*, 319.

[35]   S. Okazaki, M. Oyarna, S. Nomura, *Electroanalysis* **1997**, *9*, 1242.

[36]   M.P. Donzello, C. Ercolani, K.M. Kadish, G. Ricciardi, A. Rosa, P.A. Stuzhin, *Inorg. Chem.* **2007**, *46*, 4145.

[37]   T. Suzuki, Y. Maruyama, T. Akasaka, *J. Am. Chem. Soc.* **1994**, *116*, 1359.

[38]   M. Kumar, W. Galezowski, P.M. Kozlowski, *Int. J. Quantum Chem.* **2012**, *113*, 479.

[39]   Z.M. Xue, B. Liu, C.H. Chen, *Electrochim. Acta* **2006**, *51*, 4554.

[40]   P. Morvillo, *Sol. Energy Mater. Sol. Cells* **2009**, *93*, 1827.

[41]   K. Seto, T. Nakayama, B. Uno, *J. Phys. Chem. B* **2013**, *117*, 10834.

[42]   Y. Kawakami, A.J. Hopfinger, *J. Chem. Res. Toxicol.* **1990**, *3*, 244.

[43]   R. S. Assary, F. R. Brushett, L. A. Curtiss *RSC Adv.* **2014**, *4*, 57442.

[44]   V. Barone, M. Cossi, *J. Phys. Chem. A* **1998**, *102*, 1995.

[45]   M. Cossi, N. Rega, G. Scalmani, V. Barone, *J. Comput. Chem.* **2003**, *24*, 669.

[46]   L.I. Hernández, R. Godin, J.J. Bergkamp, M.J. Llansola Portolés, B.D. Sherman, J. Tomlin, G. Kodis, D.D. Méndez-Hernández, S. Bertolotti, C.A. Chesta, E. Mariño-Ochoa, A.L. Moore, T.A. Moore, G. Cosa, R.E. Palacios, *J. Phys. Chem. B* **2013**, *117*, 4568.

[47]   A.D. Becke, *J. Chem. Phys.* **1993**, *98*, 5648.

[48]   C. Lee, W. Yang, R.G. Parr, *Phys. Rev. B* **1988**, 37, 785.

[49]   P.C. Hariharan, J.A. Pople, *Chem. Phys. Lett.* **1972**, *16*, 217–219.

[50]   P.C. Hariharan, J.A. Pople, *Theoret. Chim. Acta* **1973**, *28*, 213.

[51]   M.M. Francl, *J. Chem. Phys.* **1982**, *77*, 3654.

[52]   M. J. Frisch, G. W. Trucks, H. B. Schlegel, G. E. Scuseria, M. A. Robb, J. R. Cheeseman, G. Scalmani, V. Barone, B. Mennucci, G. A. Petersson, H. Nakatsuji, M. Caricato, X. Li, H. P. Hratchian, A. F. Izmaylov, J. Bloino, G. Zheng, J. L. Sonnenberg, M. Hada, M. Ehara, K. Toyota, R. Fukuda, J. Hasegawa, M. Ishida, T. Nakajima, Y. Honda, O. Kitao, H. Nakai, T. Vreven, J. A. Montgomery, Jr., J. E. Peralta, F. Ogliaro, M. Bearpark, J. J. Heyd, E. Brothers, K. N. Kudin, V. N. Staroverov, R. Kobayashi, J. Normand, K. Raghavachari, A. Rendell, J. C. Burant, S. S. Iyengar, J. Tomasi, M. Cossi, N. Rega, J. M. Millam, M. Klene, J. E. Knox, J. B. Cross, V. Bakken, C. Adamo, J. Jaramillo, R. Gomperts, R. E. Stratmann, O. Yazyev, A. J. Austin, R. Cammi, C. Pomelli, J. W. Ochterski, R. L. Martin, K. Morokuma, V. G. Zakrzewski, G. A. Voth, P. Salvador, J. J. Dannenberg, S. Dapprich, A. D. Daniels, Ö. Farkas, J. B. Foresman, J. V. Ortiz, J. Cioslowski, and D. J. Fox, *Gaussian 09, Revision A.02*, Gaussian, Inc., Wallingford CT, 2009.